Advances in Machinery, Materials Science and Engineering Application IX
M. Chen et al. (Eds.)

doi:10.3233/ATDE230439

Friction Thermal Effect Analysis of High Pressure Turbine Rubbing in Aero-Engine

Ying ZHANG [a], Zitong YANG [a,1] and Xiangpeng MENG [a]
[a] *School of Aeronautical Engineering, Civil Aviation University of China, China*

Abstract. When the high-pressure turbine of an aero-engine comes into contact with friction, the friction-heat effect that results raises the temperature at the site of contact quickly. In extreme circumstances, it will harm the blades and casing and impair the engine's ability to function properly. A vane-casing thermo-solid coupling model was developed using the finite element method to study the impact of the frictional heat effect on local details at the contact point. The distribution rules of blade temperature and stress were examined when the rotational speed changed and whether the coating was applied to the casing inner surface. The findings indicate that there is a temperature asymmetry between the blade and casing and that the rubbing friction heat effect is primarily distributed on the contact surface between the blade and casing. The influence area is also small and will rise to a high temperature in a very short period. Temperature and stress are impacted by variations in rotational speed and the use of coatings. The temperature and stress peaks at blade contact can be greatly decreased by coating the inside surface of the casing. The frictional heat effect created by rubbing should be taken into account in real-world engineering issues.

Keywords. Aero-engine, High pressure turbine, blade casing, Finite element, Frictional heat effect, Ceramic coating

1. Introduction

The flight condition of an aircraft is directly impacted by the aero engine’s usual operation as a high-speed rotating precision machine. Modern aero engines will use an acceptable design of tip clearance to obtain improved working efficiency, thrust-weight ratio, and reduced fuel consumption. On engine performance, efficiency, reliability, and safety in particular, tip clearance values of high-pressure turbines under the effect of various loads during operation have a very significant role [1-4]. When the tip clearance is insufficient, friction will develop between the blades and the casing [5-7], which will result in catastrophic failures like blade wear, machine vibration, blade fracture, and igniting from a high-temperature contact surface. The literature [8-11] investigated the frictional thermal effects caused by touching and friction and found that there is an asymmetry in the frictional thermal effects between the blade and the casing. The temperature varies greatly in a short period of time, which has an effect on the vibration of the complex rotor system in addition to the temperature and mechanical properties of the contact area between the blade and the casing.

[1] Zitong YANG, Corresponding author, School of Aeronautical Engineering, Civil Aviation University of China, China; E-mail: y82399695@163.com.

The frictional force, the vibration response brought on by friction, the chaotic phenomenon in the process of friction, etc. are the main topics of research in aero-engine friction at the moment. The temperature distribution of the components and the factors impacting the frictional heat effect have not been the subject of a lot of investigation. It is important to investigate the effects of the temperature generated by the frictional heat of the blade and the magazine on the blade and the magazine through the finite element method simulation as the temperature distribution at the contact and the stress value caused by the frictional heat are difficult to measure directly by experimental equipment.

Based on the finite element method, a blade-casing frictional thermal effect model was developed in this research. According to the original size, UG NX chose a common aero-engine high-pressure turbine to create a single-blade-casing model and a multi-blade-casing model. On the models, a transient frictional thermal simulation was run. To explore the role of frictional thermal effect on temperature and stress, numerical results at the contact part between the blade and casing were obtained. These results served as a guide for real-world engineering issues.

2. Thermal Effect Theory of Contact and Friction

2.1. Blade-casing Contact Theory

An illustration of the friction between a single blade and the casing is shown in figure 1. The normal frictional force brought on by the collision of two elastomers is satisfied according to Hertz theory:

$$F_n = k_h \mu_{cr}^{3/2} \tag{1}$$

$$k_h = \frac{4}{3\left(\frac{1-\mu_1^2}{E_1} + \frac{1-\mu_2^2}{E_2}\right)} \left(\frac{R_1 R_2}{R_1 + R_2}\right)^{1/2} \tag{2}$$

In the formula: k_h —Hertz contact stiffness coefficient, According to the material properties of the parts and the geometric size of the modeling; μ_1 —is Poisson's ratio of the rotor; μ_2 —Is Poisson's ratio of the static element; E_1 —is the elastic modulus of the rotor; E_2 —is the elastic modulus of the statics; R_1 —is the curvature radius of the rotor in the contact area; R_2 —is the radius of curvature of the static ion in the contact region.

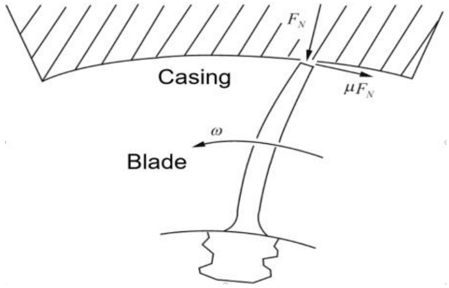

Figure 1. Schematic diagram of single blade rubbing with casing.

2.2. Frictional Heat Effect

The thermal boundary of blast-casing friction model was simplified as follows to keep the computation quantity moderate and the results similar to reality:

(1) The blade and the outside of the casing are in direct contact with the air, and convective heat transfer is the predominant method, ignoring heat loss brought on by heat radiation.

(2) Do not take into account friction in the process of material wear.

(3) All materials are isotropic.

(4) The heat transfer coefficient does not change with the temperature or spatial position of the model.

Using the aforementioned premises and the basic principle of heat transfer, the internal heat conduction equation of the model can be stated as follows:

$$K\left(\frac{\partial^2 T}{\partial r^2}+\frac{1}{r}\frac{\partial T}{\partial r}+\frac{1}{r^2}\frac{\partial^2 T}{\partial \theta^2}+\frac{\partial^2 T}{\partial z^2}\right)+\dot{Q}=0 \tag{3}$$

In the formula: K—Is the thermal conductivity coefficient; T—Temperature; $\dot{Q}$—Internal heat source density.

The friction heat source on the contact surface, which is the internal heat source in the blade-casing friction model, has the following density:

$$\dot{Q}=k_{\mu}F_{n}\omega\left(R_{d}+L\right) \tag{4}$$

In the formula: k_{μ}—Friction coefficient; F_{n}—Friction contact surface normal phase pressure; ω—Angular velocity of blade rotation; R_d—Wheel radius; L—Blade length.

3. Surface Temperature Analysis of Blade-casing Model

This section takes the single blade-casing model as the object of study, through ANSYS Workbench transient dynamics module, the blade and the magazines occur a single touch and friction failure, that is, the blade and the magazines continue to contact, not with the rotation angle changes in the process of separation, and analyze its impact on the temperature field.

3.1. Finite Element Model of Blade-Casing Friction Heat

The frictional thermal effect is a local feature brought on by the friction phenomenon, and it is a feature of the actual model of the high-pressure turbine of a typical engine that exhibits cyclic symmetry. Interactions exist between temperature and structural alterations [12]. The temperature distribution will be impacted by the contact pressure created during friction collision, and the ensuing temperature field will force the structure to expand and contract with temperature changes, leading to deformation. This condition is not met by indirect coupling. To build a local model of the frictional thermal effect of a single-bladed casing, a blade with friction and corresponding casing were chosen as the research item in this part, using a typical engine as an example and disregarding the effects of other blades. Figure 2 illustrates that the high-pressure turbine blades were given the code DZ125 and the housing the code GH907. To calculate the specific properties of materials, the direct coupling method was used in the literature [13].

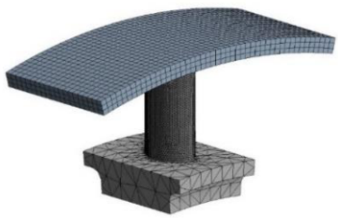

(a) Frictional thermal effect model of single blade-casing

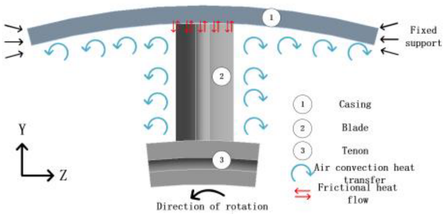

(b) Meshing of single blade-casing model

Figure 2. Finite element model of single vane casing.

Fixed restrictions were placed on the left and right end sides of the casing, and the starting temperature was set at 22°C. The total model was subjected to a convective heat transfer of 1500W/m^2°C, and the blade rotated at a speed of 3000rpm. Considering that a single rubbing lasts 0.002 seconds. To create face-surface friction contact with the inside surface of the casing, the blade's tip was chosen. The friction coefficient was set at 0.2 [10], the thermal conductivity coefficient between contact elements was set at 0.9, the thermal weight coefficient was set at 0.3, and the thermal conversion coefficient was set to the default value of 1. The temperature freedom and thermal property were increased by changing the keyword and real constant. The calculation was done using the generalized Lagrange method.

3.2. Influence of Frictional Thermal Effect on Temperature at Blade-casing Contact

The temperature distribution at the blade was obtained, as shown in figure 3, after converting the Solid186 unit with temperature freedom into the Solid226 unit with temperature freedom for computation and analysis.

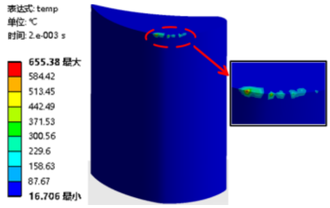

Figure 3. Temperature distribution at blade rubbing point.

The contact point between the blade and the case is the only component that is above room temperature, as seen in the above image. Several contact points as well as a single point are in touch with the casing in the contact position. From left to right, there are a total of seven contacts. Temperature values differ because the distribution of contact sites is asymmetrical and each contact point's degree of contact varies. The friction failure causes the temperature at the friction point to rising from room temperature to 655°C, the temperature gradient changes dramatically, and the thermal stress generated is easily damaging to the blade because the heat generated in the contact area cannot be transferred to the surrounding area and is concentrated near the friction point.

3.3. Analysis of Influencing Factors of Friction Thermal Effect

The blade and the cassette exist temperature asymmetry effect, compared with the cassette, the blade part is more likely to cause damage due to high temperature, this section takes the blade as an example, analyze the speed change and whether to consider the coating, the impact on the temperature place due to frictional heat generated by touching. In order to study the blade and the cassette occurrence touch friction area temperature size and distribution law, choose the blade tip as the reference surface, the blade leaf back at the circumferential arc curve as the starting point of the axial straight line to establish the path, as shown in figure 4.

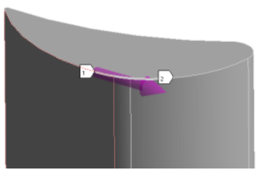

Figure 4. Schematic diagram of blade inlet edge paths.

3.3.1. Rotational Speed

The centrifugal deformation brought on by the change in rotational speed is one of the primary variables influencing the change in radial clearance, and it directly affects whether friction failure will occur during the engine's operation. The engine's tip clearance is at its lowest in the accelerated transition state, which makes friction failure easy to happen, according to the literature study [14-16]. It is known that the working speed of a typical engine in slow running conditions is approximately 9000RPM based on the relation diagram between time and speed in each typical working condition provided by MTU technical manual and literature [17]. The author equalized the speed in the acceleration process and chose three different speeds within the range of

3000RPM, 6000RPM, and 9000RPM for research. This was done to simulate the influence of the speed change on the frictional thermal effect caused by the friction fault in the transition acceleration state from engine start-up to slow train.

The temperature distribution curve in path 1 as the speed varies is shown in figure 5. This path has seven points of friction. When the path's length varies, the temperature fluctuates quickly depending on how close it is to the friction point and how far away it is from it. The temperature increases to roughly 900°C at 9000 rpm. Each node in path 1 experiences an increase in temperature as the rotational speed rises, with the temperature of the node closest to the edge of the path experiencing a little change. The location of the largest point of friction in the path is unaffected by changes in rotational speed. The temperature value at the friction point rises more abruptly when the rotational speed increases from 6000 to 9000 rpm than it does when it rises from 3000 to 6000 rpm. Thus, the friction heat effect will be more severe the faster the rotating speed increases.

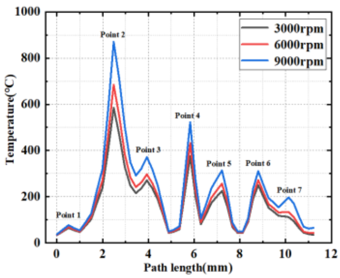

Figure 5. The temperature distribution curve at path 1 when the rotational speed changes.

3.3.2. Coating

The space between the rotor and the stator can be reduced when the high-temperature sealing coating is used on air path sealing components like the high-pressure compressor and turbine of aero engines [18]. Yttrium oxide stabilized zirconia (YSZ), a type of ceramic material, is currently utilized extensively in high-pressure turbines due to its outstanding high-temperature resistance and low thermal conductivity [19, 20].

In this study, a double-layer structural coating was chosen and applied to the casing's inner surface. The NiCoCrAlY bond layer sits between the ceramic and the matrix, which is constructed of GH907, and the surface layer is a ceramic layer formed of YSZ material. Figure 6 depicts the exact structure and material properties reference [21].

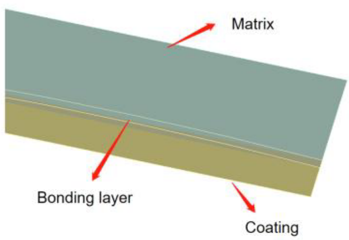

Figure 6. Schematic diagram of double-layer structure coating.

The temperature distribution curve at path 1 obtained by altering merely the rotating speed is depicted in figure 7 when the ceramic coating is applied. The temperature differential at path 1 greatly lowers after taking the coating into account, and the distribution trend is similar to that before taking the coating into account, as can be seen in the picture. The maximum contact point moved from contact point two to contact point six as the number of contact points increased from seven to six. However, both the number of contact points and the position of the maximum contact points have an effect. Following coating, the temperatures at the two friction sites were much lower than before, while the temperatures at the other six friction points were slightly higher than before but still lower than the temperature at the two friction points.

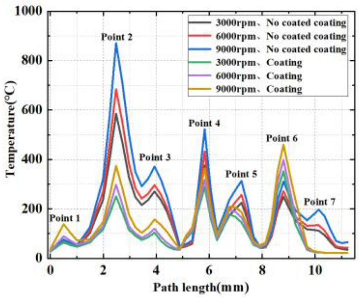

Figure 7. Temperature distribution curve at path 1 when speed changes.

4. Stress Analysis of the Blade-casing Model

When the frictional thermal effect is considered, the contact surface of the blade and the cassette increases the thermal stress caused by the frictional thermal effect, resulting in a further increase in the stress on the contact surface, and this section studies its effect on the stress by comparing the results when the frictional thermal effect is considered or not.

4.1. Influence of Friction Heat Effect on Stress at Blade Contact

The stress field of the blade obtained in the coupled field is shown in figure 8 (a). The upper half is the stress distribution at the leaf basin and leaf back, the lower half is the stress distribution at the tip of the blade, the results show that: the stress is mainly concentrated in the leaf basin, leaf back and the tip of the blade and the cassette contact area, the stress value at the blade touch mo point two is the largest, and the highest temperature when the coating is not considered touch mo point to maintain consistency. The stress distribution at the leaf basin and leaf back in the structural field is similar to that in figure 8(a), but the stress distribution at the tip of the blade changes, as shown in figure 8 (b), in the absence of frictional heat effect on the structure, there is only one point between the blade and the magazine where the touching occurs, and the stress is mainly concentrated near the touching point.

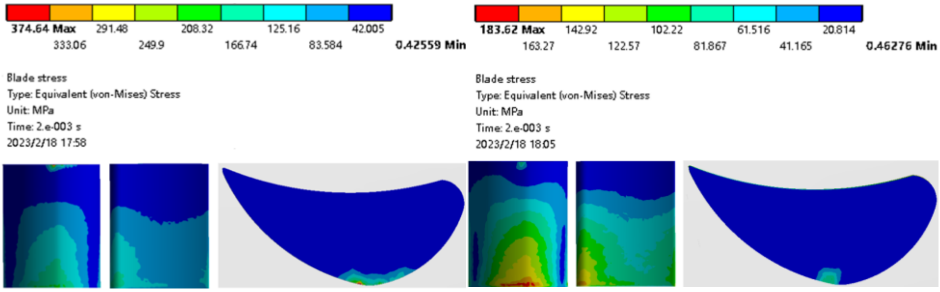

(a) Stress distribution in the coupling field (b) Stress distribution in the structural field

Figure 8. Blade stress distribution under different conditions.

5. Simulation Analysis of Friction Process of Multi-blade and Casing models

In order to analyze the effects of multiple frictional frictions on the temperature and stress distribution of blades during high-speed rotation and to validate the findings of the previously mentioned single frictional friction, a frictional thermal effect model of multi-blade and casing frictional friction was established.

5.1. Finite Element Model

The model is appropriately simplified to lower the calculation volume. A baffle in the shape of a circle replaces the tenon. The wheel disk is reduced to a rigid housing because the impact on the blade temperature during the occurrence of the touch-and-go problem is primarily studied [22] and the radial stiffness of the wheel disk is greater than the blade. To improve the temperature degrees of freedom, the C3D8T cell is utilized to mesh the turbine blade, the wheel disk, and the cassette with a hexahedral mesh. Figure 9 illustrates the completed mesh model of the blade-magazine structure. The same materials used in Section 3 were chosen.

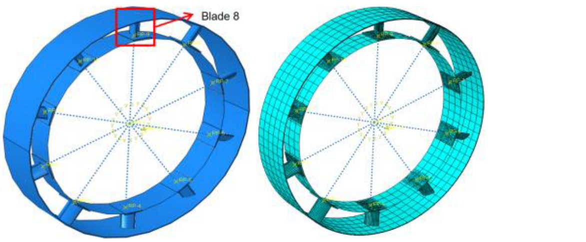

(a)Multi-blade-casing 3D model (b)Meshing of multi-blade-casing model

Figure 9. Finite element model of multi-blade casing.

In order to consider both the inertial effects caused by the rotating centrifugal force and the nonlinear response due to the touching friction, an implicit-explicit sequential solution is performed for the whole system. The implicit algorithm is used to calculate the steady-state response of the rotor blade system under centrifugal force, and then the results are imported into the explicit solver in the form of preloads for solving the bump-friction process. The lower surface of the cassette is defined as the first plane and the upper surface of the blade as the second plane, and the penalty function method is chosen to set the friction coefficient constant at 0.2. The cassette is fixedly restrained at both ends, the blade disc structure is elastically supported, and the blade part of the disc is bound to the disc by the baffle plate. Based on the implicit analysis, an initial velocity of 314 rad/s is applied to the blade and the wheel at the moment of 0, followed by an acceleration to 1256 rad/s within 0.001 s. The subsequent time is maintained at the rated speed for stable operation, and the total simulation time is 0.011 s.

5.2. Rubbing Process of Multi-Blade-Casing Model

Taking blade 8 as an example, after the simulation calculation by implicit-explicit dynamics, the temperature change of the tip part at different times is obtained as shown in figure 10, and the distribution trend is consistent with the analysis results in Section 4. With the increase of the number of touching and the change of the degree of touching, the temperature gradually increases and the temperature field gradually spreads around the touching point.

In order to study the relationship between the temperature trend and the frictional heat flow, the time domain curve of temperature-frictional heat flow at the maximum touching point was plotted as shown in figure 11. From the figure, it can be seen that the temperature change with time shows a "sawtooth" rise, which is caused by the alternating effect of heat flow input and convective heat transfer. The heat flow density trend is consistent with the temperature, and the heat flow rate is always greater than zero.

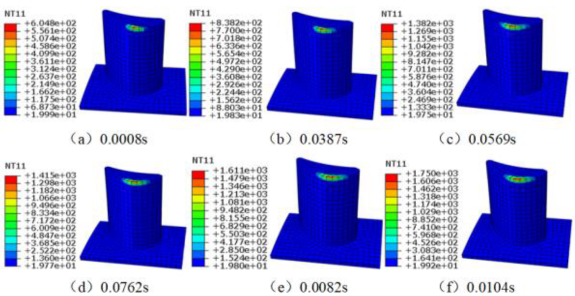

Figure 10. Blade temperature distribution at different times.

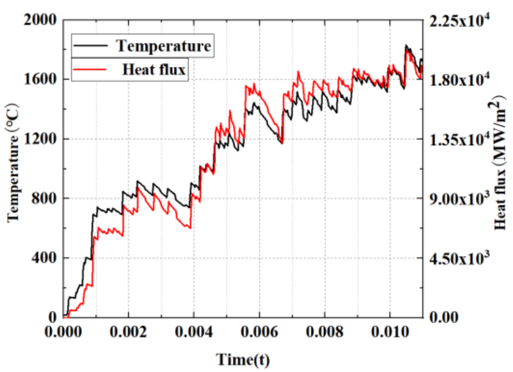

Figure 11. Time-domain curve of temperature and heat flux.

6. Conclusion

The following conclusions are reached by developing a finite element model of the thermal effect of blade-magazine friction, researching the impact of various influencing factors and variations in the number of friction on temperature rise and stress conditions at the blade friction point as well as the distribution pattern of temperature and stress:

(1) In the blade-magazine model, when friction occurs, there are multiple friction points and the distribution of the friction points is not regular, and the temperature near the friction points rises rapidly under the influence of frictional heat effect. When the rotational speed changes, it will cause the temperature to increase, but it does not affect the location of the touching point.

(2) The stress at the blade is also concentrated in the vicinity of the touching point, when the frictional thermal effect is not considered, there is only one touching point between the blade and the cassette, after consideration because of the temperature load on the blade structure, so that the touching point increases, and then lead to the change of the stress distribution trend at the blade. Under the action of thermal stress, the stress value at the touch point increases, and the change is more dramatic.

(3) The application of ceramic coating makes the position of the maximum friction point change, so that the temperature of the original maximum friction point is greatly reduced, and the temperature of the new maximum friction point is increased, but it is still smaller than the result when the coating is not applied. In order to avoid frictional failure at the high-pressure turbine, in addition to considering the active control technology of blade tip clearance, the application of ceramic coating can also solve the failure caused by frictional heat effect, so that the engine performance, safety and service life are improved.

(4) With the change of the number of friction, the temperature of the blade friction point is affected by the heat flow density input shows a "sawtooth" rising trend, the heat flow density change pattern is consistent with the temperature, and the heat flow rate is always greater than zero.

References

[1] Kypuros JA, Melcher KJ. A Reduced Model for Prediction of Thermal and Rotational Effects on Turbine. NASA/TM-2003-212226, 2003.

[2] Zhan JZ, Zhang G, Song WY, et al. Theoretical analysis and numerical simulation of tip clearance in 12-stage rotor of a high-pressure compressor. Mechanical Science and Technology for Aerospace Engineering. 2019; 38(10):1632-1640. DOI:10.13433/j.cnki.1003-8728.20190003.

[3] Cao HL, Wang H. Aircraft engine of uneven tip clearance under the hot solid coupling analysis. Journal of mechanical design. 2019; 4(10): 80-85. DOI: 10.13841/j.carolcarrollnki JXSJ. 2019.10.013.

[4] Qiao WY, Luo HL, Xu KF. Analytical study of turbine blade tip clearance loss model. Mechanical Design and Manufacture. 2006; (10):180-182.

[5] Chen G, Feng GQ, Jiang GY, et al. Analysis and verification of vibration acceleration characteristics of aeroengine vane casing for rubbing fault. Aircraft Engine. 2014; 40 (01): 16 + 10-78 DOI: 10.13477 / j.carol carroll nki aeroengine. 2014.01.002.

[6] Liu Y, Tai XY, Chen YZ, et al. Nonlinear oil film force under the action of rubbing rotor system dynamics analysis. Journal of Mechanical Design and Manufacturing, 2013; (3): 35+37. DOI: 10.19356 / j.carol carroll nki. 1001-3997.2013.03.012.

[7] Jin YL, Liu ZW, Chen YS. Simulation of Friction Fault of aero-engine Double-rotor blade-Casing. Acta Aeronautica et Astronautica Sinica. 2022; 1-13.

[8] Kennedy, FE. Single pass rub phenomena - Analysis and experiment. Journal of Tribology. 1982; 104(4):582-588.

[9] Zhu XZ, Yuan HQ, Li D. Friction heat effect of aviation engine high-pressure rotor rubbing responses of the system. Journal of Propulsion Technology. 2010; 31(3): 366-371. The DOI: 10.13675 / j.carol carroll nki TJJS. 2010.03.017.

[10] Lai MG, Li SM, Wen J. Aircraft engine blade - casing rubbing friction heat effect simulation analysis. Journal of Aircraft Engine. 2017;(01): 21-26. DOI: 10.13477 / j.carol carroll nki aeroengine. 2017.01.005.

[11] Liu MJ, Dong Y, Yang GJ. Study on asymmetric thermal effect and temperature rise curve of aero-engine blade/casing rubbing. Materials Advances in China. 2021; 40(07):542-547.

[12] Wang LL, Li SM, Lai MG, et al. Thermal coupling simulation of aero-engine vane casing. Chinese Journal of Applied Mechanics. 2016;33(06):1045-1050+1122.

[13] Huang BY. China Materials Engineering (Volume 4) Nonferrous Metal Materials Engineering (I). Chemical Industry Press, 2006.

[14] Guo SF, Xu B. The influence of temperature and rotational speed of turbine blade tip radial clearance. Journal of Propulsion Technology. 2000; (04): 51-53. DOI: 10.13675 / j.carol carroll nki TJJS. 2000.04.017.

[15] Qi WK, Chen W. Numerical analysis of tip clearance in high pressure turbine of an aero-engine. Journal of Nanjing University of Aeronautics and Astronautics. 2003; (01): 63-67.DOI:10.16356/ J.1005-2615.2003.01.013.

[16] He Hi, Mao JK, Liu FY, et al. Considering engine performance degradation of turbine blade tip clearance forecast method research. Journal of Propulsion Technology. 2020; 9 (10): 2283-2291. The DOI: 10.13675 / j.carol carroll nki TJJS. 190680

[17] Niu DS. Numerical analysis of turbine tip clearance and size conversion method of cold and hot state. Nanjing University of Aeronautics and Astronautics, 2004.

[18] General Editorial Committee of Aeroengine Design Manual. Aeroengine Design Manual (Volume 10). Beijing: Aviation Industry Press, 2001.

[19] Zhang JH, Song KQ, Zhang M, et al. High performance ceramic coating and its development trend of preparation technology. Journal of Surface Technology. 2017; 46-48 (12) : 96-103. The DOI: 10.16490 / j.carol carroll nki. Issn 1001-3660.2017.12.017.

[20] Cheng TT, Wang ZP, Dai SJ, et al. Research progress of ceramic based high temperature sealing coatings for aero engines. Chinese Journal of Mechanical Engineering. 2021; 57(10):126-136+147.

[21] RANJBAR-FARM, ABSIA J, SHAHIDIB S, et al. Impact of the non-homogenous temperature distribution and the coatings process modeling on the thermal barrier coatings system. Materials and Design. 2011; 32 (2): 728-735.

[22] Liu SG, Hong J, Chen M. Aircraft engine blade - for the numerical simulation of the rubbing process. Journal of Air Power. 2011; 26 (6): 1282-1288. The DOI: 10.13224 / j.carol carroll nki jasp. 2011.06.01.